AL- Taqani ,Vol . 26 , No 2 ,2013

NATURAL CONVECTIVE ENHANCEMENT IN A RECTANGULAR [+]ENCLOSURE FILLED WITH NANOFLUID

Selah M. Salih [*]

Abstract:

Heat convective enhancement in a two-dimensional rectangular enclosure utilizing nanofluids is investigated. The basic fluid in the enclosure is an ethylene glycol-based nanofluid containing (Cu, CuO, AL_2O_3 , or TiO_2) nanoparticles. Calculations of heat transfer rates were performed for a range of Rayleigh number ($10^3 \le Ra \le 10^6$), Prandtl number is taken as (Pr = 204), and solid volume fraction ($0.01 \le \phi \le 0.04$). The effects of Rayleigh number and solid volume fraction for different nanofluids on hydrodynamic and thermal characteristics are investigated. Results are presented in the form of streamline and isotherm plots as well as the velocity profiles and the variation of local and mean Nusselt number of rectangular enclosure utilizing nanofluids. The results indicate that the effects of solid volume fraction grow stronger on the heat transfer rates for nanoparticles. In addition, the increases of Rayleigh number leads to decrease the solid concentration effect. Also, the incremental change in the average Nusselt number is strongly depending on the nanoparticles chosen. Comparisons with previously published work on the basis of special cases are performed and found to be in excellent agreement with in maximum error (± 4 %).

تعزيز الحمل الحراري الطبيعي لحيز مغلق مستطيل الشكل باستخدام مائع نانوي

صلاح مهدي صالح

المستخلص:

تم إجراء دراسة عددية لزيادة الحمل الحراري الطبيعي لحيز مغلق مستطيل الشكل ثنائي البعد مملوء بمائع نانوي. تم أختبار المادة السائلة (أثيلين كلآيكول) موضوعة مع جسيمات دقيقة جدا مثل (النحاس، اكسيد النحاس، أكسيد الألمنيوم، أو أكسيد التيتانيوم). تم تمثيل النتائج العددية لمعدلات انتقال الحرارة لعدد رالي في المدى ($10^3 \le Ra \le 10^6$)، إخذ عدد برانتل (Pr = 204) ، و التركيز الحجمي ($0.01 \le \phi \le 0.04$). تم دراسة تأثير عدد رالي و التركيز الحجمي على خصائص سلوك الجريان والحرارة. تم تمثيل نتائج الدراسة بدلالة خطوط الانسياب و خطوط درجات الحرارة الثابتة بالإضافة، إلى رسومات بيانية أخرى للسرعة وعدد نسلت الموقعي والمعدل للحيز المستطيل المغلق باستخدام مائع نانوي. بينت النتائج ان معدل انتقال الحرارة يزداد بقوة بزيادة التركيز الحجمي للمائع النانوي للجسيمات الدقيقة. بالإضافة، ان زيادة عدد رالي يقلل من تأثير التركيز الحجمي. كذلك ، كمية الزيادة لمعدل عدد نسلت تكون معتمدة بقوة على نوع الجسيمات الدقيقة المختارة . تم مقارنة النتائج العددية للدراسة الحالية مع دراسات سابقة عند نفس الظروف الحدية وكانت مقبولة و متقاربة بنسبة خطأ (±4%).

[+] Received on 11/4/2012 , Accepted on 6/5/2013 .
[*]Assit Lech . / Technical College – Najaf

Introduction:

The augmentation of heat transfer in the field of Nanotechnology is considered to be one of the most important inventions in this century. Convective heat transfer in a rectangular cavity with adiabatic horizontal walls and isothermal vertical walls are a prototype of many industrial applications, such as electronic cooling, transportation, the environment and national security. Nanofluids exhibit superior heat transfer properties in comparison with conventional heat transfer fluids. It refers to a two phase mixture that is composed of saturated liquid and extremely fine metallic particles called nanoparticles. The suspended ultra fine particles change transport properties and heat transfer performance. The thermal conductivity is strongly dependent on the solid volume fraction and properties of nanofluids. Enhancement of heat transfer in these systems is an essential topic from an energy saving perspective. The low thermal conductivity of convectional heat transfer fluids such as water and oils is a primary limitation in enhancing the performance and the compactness of such systems. An innovative technique to improve heat transfer is by using nano-scale particles in the base fluid. Nanotechnology has been widely used in industry since materials with sizes of nanometers possess unique physical and chemical properties. Nano-scale particle added fluids are called as nanofluid which is firstly utilized by Choi, [1].

In the literature, various studies have been published on the mechanism of natural convection in differentially heated cavities with different geometrical parameters and boundary conditions. The effects of transport properties of the nanofluid and thermal dispersion are included, Xuan, [2]. The natural convection heat transfer and fluid flow of two heated partitions within an enclosure, and the effect of locations and sizes of partitions on heat transfer and fluid was studied, Dagtekin, and Oztop, [3].

The thermal conductivity increases of nanofluids are due to Brownian motion of particles, molecular-level layering of the liquid at the liquid/ particle interface, the nature of heat transport in the nanoparticles, and the effect of nanoparticle clustering , Keblinski et al., [4]. The first investigation of the problem of buoyancy-driven heat transfer enhancement of nanofluids in a two-dimensional enclosure. The results illustrated that the nanofluid heat transfer rate increases with an increase in the nanoparticle volume fraction, Khanafer et al., [5]. The computational studies investigated of the natural convection in a differentially heated, partitioned, and square cavity containing heat generating fluid studied by, Oztop, and Bilgen, [6].

Hwang et al., [7] conducted the buoyancy-driven heat transfer of water-based (Al_2O_3) nanofluids in a rectangular cavity was investigated. They showed that the ratio of heat transfer coefficient of nanofluids to that of base fluid is decreased as the size of nanoparticles increases, or the average temperature of nanofluids is decreased. Jou, and Tzeng, [8] accomplished a numerical study of the natural convection heat transfer in a rectangular enclosure by using nanofluids to enhance. They indicated that volume fraction of nanofluids cause an increase in the average heat transfer coefficient. The computational studies reported in this area include a single-phase model, in which solid particles are considered to behave as fluids, because the nanoparticles are easy fluidized ,(Tiwari, and Das, [9] ; Oztop, and Abu-Nada, [10] ; Abu-Nada, and Oztop, [11] ; and Lin, and Violi, [12]).

The analysis of heat transfer and fluid flow of natural convection in a cavity filled with (AL_2O_3)-water nanofluid that operates under differentially heated walls was tested by, Lin, and Violi, [12]. They showed that the decreasing in the Prandtl number results in amplifying the effects of nanoparticles due to increased effective thermal diffusivity.

The main aim of this study is to examine the natural convection heat transfer enhancement in a differentially heated rectangular enclosure filled with nanofluids. In this work is taken base fluid ethylene glycol (EG) based nanofluid containing four different type of nanoparticles:

(Cu, CuO, AL_2O_3 , and TiO_2) are tested to provide a more unifying picture of the various pertinent parameters on heat transfer characteristics of nanofluids within a rectangular enclosure.

Mathematical Formulation:

Consider a steady two-dimensional flow inside a square enclosure filled with nanofluid. In the present problem, the mathematical equations describing the physical model are based on the following assumptions:

I. In the enclosure, the horizontal walls are insulated, and impermeable to mass transfer.

II. The vertical walls are differentially heated, both walls are isothermal at (T_{ho}) and (T_{co}) respectively, ($T_{ho} > T_{co}$).

III. The base fluid (EG) and the solid spherical nanoparticles (Cu, CuO, AL_2O_3 , and TiO_2) are in thermal equilibrium.

IV. The thermo-physical properties of the nanofluid are assumed constant except for a variation of the density which is determined based on Boussinesq approximation.

V. The nanofluid in the enclosure is Newtonian, incompressible and laminar.

VI. Radiation heat transfer between the sides of the enclosure is negligible when compared with the other mode of heat transfer.

VII. **Table 1** presents the thermo-physical properties for the base fluid and the different nanoparticles.

The geometric and the cartesian coordinate system are schematically shown in **Fig. 1**. Under the above assumptions, the governing equations in dimensional form used in the present study are, Lin, and Violi, [12]:

Continuity equation:

$$\frac{\partial u}{\partial x}+\frac{\partial v}{\partial y}=0 \tag{1}$$

x-momentum equation:

$$u\frac{\partial u}{\partial x}+v\frac{\partial u}{\partial y}=-\frac{1}{\rho_{nf}}\frac{\partial p}{\partial x}+\frac{\mu_{eff}}{\rho_{nf}}\left(\frac{\partial^2 u}{\partial x^2}+\frac{\partial^2 u}{\partial y^2}\right) \tag{2}$$

y-momentum equation:

$$u\frac{\partial v}{\partial x}+v\frac{\partial v}{\partial y}=-\frac{1}{\rho_{nf}}\frac{\partial p}{\partial y}+\frac{\mu_{eff}}{\rho_{nf}}\left(\frac{\partial^2 v}{\partial x^2}+\frac{\partial^2 v}{\partial y^2}\right)+\frac{1}{\rho_{nf}}\left[(1-\phi)\rho_f\beta_f+\phi\rho_s\beta_s\right]g\left(T-T_{co}\right) \tag{3}$$

Energy equation:

$$u\frac{\partial T}{\partial x}+v\frac{\partial T}{\partial y}=\alpha_{nf}\left(\frac{\partial^2 T}{\partial x^2}+\frac{\partial^2 T}{\partial y^2}\right) \tag{4}$$

Where (α_{nf}), the effective of theral diffusivity is defined as: $\alpha_{nf}=\dfrac{k_{eff}}{(\rho c_p)_{nf}}$

Vorticity equation and components of velocities :

$$\omega = \frac{\partial v}{\partial x} - \frac{\partial u}{\partial y}, \quad u = \frac{\partial \psi}{\partial y}, \quad v = -\frac{\partial \psi}{\partial x} \tag{5}$$

The effective density of a fluid containing suspended particles is given by, Oztop, and Abu-Nada, [10]:

$$\rho_{nf} = (1-\phi)\rho_f + \phi\rho_s \tag{6}$$

The heat capacitance of the nanofluid is expressed as, Oztop, and Abu-Nada, [10]; and Lin, and Violi, [12] :

$$(\rho c_p)_{nf} = (1-\phi)(\rho c_p)_f + \phi(\rho c_p)_s \tag{7}$$

The effective thermal conductivity of the nanofluid is approximated by the Maxwell–Garnetts model, Oztop, and Abu-Nada, [10] :

$$k_{eff} = \frac{k_{nf}}{k_f} = \frac{k_s + 2k_f - 2\phi(k_f - k_s)}{k_s + 2k_f + \phi(k_f - k_s)} \tag{8}$$

Moreover ,the effective dynamic viscosity of the nanofluid which is given by Brinkman ,[13]:

$$\mu_{nf} = \frac{\mu_f}{(1-\phi)^{2.5}} \tag{9}$$

The following dimensionless groups based on length of enclosure (L) are introduced:

$$\begin{gathered} X = \frac{x}{L}; \quad Y = \frac{y}{L}; \quad \Omega = \frac{\omega L^2}{\alpha_f}; \quad \Psi = \frac{\psi}{\alpha_f}; \quad U = \frac{uL}{\alpha_f}; \quad V = \frac{vL}{\alpha_f}; \\ \theta = \frac{T - T_{co}}{T_{ho} - T_{co}}; \quad Ra = \frac{g\beta_f \rho_f (T_{ho} - T_{co}) L^3}{\mu_f \alpha_f}; \quad \Pr = \frac{\mu_f}{\rho_f \alpha_f} \end{gathered} \tag{10}$$

By using the dimensionless parameters, the governing momentum, energy, and vorticity equations in terms of the stream function-vorticity formulation are written as, respectively:

$$\begin{aligned} \frac{\partial \Omega}{\partial X}\frac{\partial \Psi}{\partial Y} - \frac{\partial \Omega}{\partial Y}\frac{\partial \Psi}{\partial X} = &\left[\frac{\Pr}{(1-\phi)^{2.5}\left((1-\phi) + \phi\dfrac{\rho_s}{\rho_f}\right)}\right]\left(\frac{\partial^2 \Omega}{\partial X^2} + \frac{\partial^2 \Omega}{\partial Y^2}\right) \\ &+ Ra \Pr\left[\frac{1}{\dfrac{(1-\phi)}{\phi}\dfrac{\rho_f}{\rho_s} + 1}\frac{\beta_s}{\beta_f} + \frac{1}{\dfrac{\phi}{(1-\phi)}\dfrac{\rho_s}{\rho_f} + 1}\right]\left(\frac{\partial \theta}{\partial X}\right) \end{aligned} \tag{11}$$

$$\frac{\partial\theta}{\partial X}\frac{\partial\Psi}{\partial Y}-\frac{\partial\theta}{\partial Y}\frac{\partial\Psi}{\partial X}=\left[\frac{k_{eff}}{(1-\phi)+\phi\dfrac{(\rho c_p)_s}{(\rho c_p)_f}}\right]\left(\frac{\partial^2\theta}{\partial X^2}+\frac{\partial^2\theta}{\partial Y^2}\right) \quad (12)$$

$$\Omega=\frac{\partial V}{\partial X}-\frac{\partial U}{\partial Y}=-\left(\frac{\partial^2\Psi}{\partial X^2}+\frac{\partial^2\Psi}{\partial Y^2}\right) \quad (13)$$

The dimensionless form of the boundary conditions is given by:

1- On the left wall (hot) *for* $X=0;\quad 0\le Y\le 2$

$$\Psi=0;\quad \Omega=-\frac{\partial^2\Psi}{\partial X^2}\quad ;\quad \theta=1$$

2- On the right wall (cold) *for* $X=1;\quad 0\le Y\le 2$

$$\Psi=0;\quad \Omega=-\frac{\partial^2\Psi}{\partial X^2}\quad ;\quad \theta=0$$

3- On the top and bottom walls

a- at top wall insulated *for* $Y=2;\quad 0\le X\le 1$ (14)

$$\Psi=0;\quad \Omega=-\frac{\partial^2\Psi}{\partial Y^2}\quad ;\quad \frac{\partial\theta}{\partial Y}=0$$

b- at bottom wall insulated *for* $Y=0;\quad 0\le X\le 1$

$$\Psi=0;\quad \Omega=-\frac{\partial^2\Psi}{\partial Y^2}\quad ;\quad \frac{\partial\theta}{\partial Y}=0$$

Nusselt Number:

The Nusselt number (Nu) depends on a number of factors such as thermal conductivity, heat capacitance, viscosity, flow structure of nanofluids, dimensions, and fractal distributions of nanoparticles. The local variation of the Nusselt number of the fluid can be expressed as:

$$Nu_y=\frac{h_{con}L}{k_f} \quad (15)$$

The local heat transfer coefficient is expressed as:

$$h_{con}=\frac{q_w}{(T_{ho}-T_{co})} \quad (16)$$

The thermal conductivity is expressed as:

$$k_{nf} = -\frac{q_w}{\partial T / \partial x} \tag{17}$$

By substituting eqs. (16), (17), and (8) into eq. (15), and using the dimensionless quantities, the local Nusselt number (Nu_y) on the left wall is written as:

$$Nu_y = -\left(\frac{k_{nf}}{k_f}\right) \partial\theta / \partial X \tag{18}$$

The heat transfer rate at the hot wall of the enclosure is presented by means of the Nusselt number (Nu), which is evaluated as follows:

$$Nu = \int_0^2 Nu_y dY \tag{19}$$

A 1/3rd Simpson's rule of integration is used to evaluate eq. (19).

Numerical Method and Validation:

The solution of the dimensionless governing eqs.(11) –(13) with the boundary conditions (eq. (14)) was obtained by using a finite difference scheme. Central difference quotients were used to approximate the second derivatives in both the (X, and Y) directions. A forward – backward technique was used for uniformly grid distributed to get a stable and converged solution for vorticity and energy equations. The solution procedure starts by supplying initial guesses of the stream function, vorticity and temperature then computes a converged solution by a Gauss–Seidel iteration technique. The numerical method was implemented in a FORTRAN language program was build to execute all the numerical steps, for the rectangular enclosure.

The solution procedure is iterated until the following convergence criterion is satisfied:

$$\tau = \frac{\sum_{i=1}^{i=M} \sum_{j=1}^{j=N} \left| \lambda^{r+1}{}_{i,j} - \lambda^{r}{}_{i,j} \right|}{\sum_{i=1}^{i=M} \sum_{j=1}^{j=N} \left| \lambda^{r+1}{}_{i,j} \right|} \le 10^{-5} \tag{20}$$

where (τ)is the tolerance; (M, and N) are the number of grid points in the (x, and y) directions, respectively, and (λ) stands for either(Ψ, Ω or θ); (r) denotes the iteration step.
Table 2 shows an accuracy test using the finite diference method using five sets of grids:(11×21, 21×41, 31×61, and 41×81). There is a good agreement found between (21×41) to (41×81) grids. Therefore, a (41×81) grid is chosen to calculate the flow and heat transfer behavior over the range of operational parameter values considered.

To ensure the accuracy and validity of the new model, a system composed of pure fluid in an enclosure analysis with (Pr = 0.7), and different (Ra) numbers is used. This system has been studied by other research groups, including Tiwari and Das, 2007, [9] ; and K.C.Lin, A Violi, 2010, [12]. **Table 3** shows the comparison between the results obtained with the present work and the values presented in the literature. The quantitative comparisons for the average Nusselt numbers along the hot wall and the maximum velocity values and their corresponding locations indicate an excellent agreement with in maximum error (±4%) for Ra=10^4. In addition, investigation of differentially heated rectangular enclosure with (Pr = 0.7), and different (Ra) numbers can be compared the average Nusselt number obtained of the present study with the results reported in the literature by Tiwari, and Das, 2007, [9]; Abu-Nada, 2008, [10]; Abu-Nada, and Oztop, 2009, [11]; and Lin, and Violi, 2010, [12]. It is clear that the present code is in good agreement with other work reported in literature as shown in **Fig. 2**.

Results And Discussion:

A numerical study is performed to investigate the natural convective flow and heat transfer characteristics of ethylene glycol-based nanofluids with various nanoparticles of different volume fractions in a rectangular enclosure. In this study was taken as (Ar = 2) rectangular enclosure, the value of Prandtl number for the base fluid (ethylene glycol) is taken to be (204). Computations are carried out for the Rayleigh number ranging from (10^3 to 10^6), and the volume fraction of nanoparticles between (0 - 4%).

The results obtained are discussed under different combinations of pertinent parameters involved in the study. **Fig. 3** (a)-(c) shows a comparison between (CuO-EG) nanofluid (plotted by dashed lines) and pure fluid (plotted by solid lines) on streamlines (on the top) and isotherms (on the bottom) for different values of Rayleigh number. The flow pattern consists of a single cell occupying the whole enclosure. The core region of the cell is at the middle of the enclosure when Ra =10^3. Here, convection is weakened and conduction is the dominant mode of heat transfer. The core region of the nanofluid is reduced compared to pure fluid for all values of Rayleigh number, the minimum value of stream function changes from (−2.6 to −22) at Ra =10^3, Ra =10^4 , and Ra =10^5, respectively. When the Rayleigh number increases, the core region of the cell moves towards the cold wall and elongates. The corresponding isotherms show a vertical temperature stratification in the core region of the rectangular enclosure.

It is clear that the flow strength and the temperature isotherms are influenced by the presence of nanoparticles. For lower values of (Ra), the flow strength is higher for (CuO) than pure fluid (EG). The core region moves towards the top-right corner of the enclosure when Ra =10^5. The isotherms cluster along the thermally active walls due to stronger circulation appear for both horizontal and vertical fluid layer. For higher Rayleigh numbers, natural convection become more vigorous and the fluid moves faster and the isotherms become more packed next to adiabatic walls.

The effect of the volume fraction on the streamlines and isotherms of nanofluid for (Cu-EG) nanofluid at (Ra =10^4) is shown in **Fig. 4**. It is found that, the fluid forms a clockwise circular cell with (Ψmin=−12) at (□=0.01). This cell was generated by the lid. Also, presence of a heat source at the left wall of the enclosure helps the cell to stretch vertically beside position of the heat source. Increasing in solid volume fraction causes in a decreasing the intensity of buoyancy and hence the flow intensity so that, the minimum value of stream function changes from (−14 to −15) at □=0.02 , □=0.03, respectively. Overall observation of **Fig.4** shows that as the volume fraction increases, movements of particles become irregular and random due to increasing of energy exchange rates in the fluid. The corresponding isotherms exhibit the characteristics of conduction dominated regime since they are distributed approximately parallel to the vertical walls. Isotherms show that temperature gradients near the hot and cold walls become more severe. For (□=0.01 to 0.03), the streamlines elongate parallel to the horizontal wall for pure fluid. It is clear that the difference between **Fig.4(b)** , and **Fig. 4(c)** from the change of the values of minimum stream flow of purefluid and nanofluid.

The variation of local Nusselt number is illustrated along the heated wall in **Fig. 5** using different nanoparticles. Values of local Nusselt number have higher values at onset of heating due to high temperature difference. Again, the highest local Nusselt number values were formed for (Cu) and the lowest one for pure fluid.

Figure(6) presents the horizontal velocity profiles along the mid-section (middle plane) of the rectangular enclosure using different nanofluids at ($Ra = 10^4$), and (□=0.02). The velocity profile shows a parabolic variation near the insulated walls. The horizontal velocity is sensitive to the type of nanoparticles for four types of nanoparticles show different horizontal velocity . However, the horizontal velocity of nanofluid is lower than that of pure fluid at the hot side and higher at the cold side. It means that particle suspension affects the flow field. The flow velocity is almost zero around the center of the enclosure. The profile also gives idea on flow rotation direction.

To show that nanofluids behave more like a fluid than the conventional solid–fluid mixture, a comparison of the isotherm and the velocity profiles is conducted inside a thermal rectangular enclosure with isothermal vertical walls at various Rayleigh numbers and volume fractions for (Cu-EG) nanofluids as shown in **Fig. 7**.

Figure illustrates the effect of Rayleigh number and the volume fraction on the isotherms and the velocity profiles at the mid-sections of the rectangular enclosure for ethylene glycol with a Prandtl number of (204). The numerical results of the present study indicate that the heat transfer feature of a nanofluid increases remarkably with the volume fraction of nanoparticles. As the volume fraction increases, irregular and random movements of particles increases energy exchange rates in the fluid and consequently enhances the thermal dispersion in the flow of nanofluid. In addition, the velocities at the center of the enclosure for higher values of Rayleigh number are very small compared with those at the boundaries where the fluid is moving at higher velocities. This behavior is also present for a single-phase flow.

The isotherms in Figure show that the vertical stratification of the isotherms breaks down with an increase in the volume fraction for higher Rayleigh numbers. This is due to a number of effects such as gravity, Brownian motion, ballistic phonon transport, layering at the solid/liquid interface, clustering of nanoparticles, and dispersion effect. In this study consider only the effect of dispersion that may coexist in the main flow of a nanofluid.

As the volume fraction increases, the velocity components of nanofluid increase as a result of an increase in the energy transport through the fluid. High velocity peaks of the vertical velocity component are shown in this figure at high volume fractions. The effect of an increase in the volume fraction on the velocity and temperature gradients along the centerline of the enclosure is shown in **Fig. 7.**

Finally, **Fig. 8** presents the variation of mean Nusselt number with volume fraction using different nanoparticles and different values of Rayleigh number. The figure shows that the heat transfer increases almost monotonically with increasing the volume fraction for all Rayleigh numbers and nanofluids. For ($Ra = 10^4$), **(Fig. 8(a)),** the lowest heat transfer was obtained for (TiO_2) due to domination of conduction mode of heat transfer since (TiO_2) has the lowest value of thermal conductivity compared to (Cu, CuO and Al_2O_3). However, the difference in the values of (Al_2O_3 , CuO, and Cu) is negligible.

The thermal conductivity of (Al_2O_3) is approximately one tenth of (Cu), as given in **Table 1**. However, a unique property of (TiO_2) is its low thermal diffusivity, **Table 1**. The reduced value of thermal diffusivity leads to higher temperature gradients and, therefore, higher enhancements in heat transfer. The (Cu) nanoparticles have high values of thermal diffusivity and, therefore, this reduces temperature gradients which will affect the performance of (Cu) nanoparticles. As volume fraction of nanoparticles increases, difference for mean Nusselt number becomes larger especially at higher Rayleigh numbers due to increasing of domination of convection mode of heat transfer. The highest heat transfer is recorded when using (Cu)-nanofluids.

Conclusion:

Heat transfer enhancement in a two-dimensional rectangular enclosure filled with various nanofluids is studied numerically for a range of Rayleigh numbers and volume fractions. The present results illustrate that the suspended nanoparticles substantially increase the heat transfer rate at any given Rayleigh number. In addition, the results illustrate that the nanofluid heat transfer rate increases with an increase in the nanoparticles volume fraction. The presence of nanoparticles in the fluid is found to alter the structure of the fluid flow. A comparative study of different models based on the physical properties of nanofluid is analyzed in detail. The variances among these models are analyzed in the present study. However, the incremental change in the average Nusselt number is strongly depending on the nanoparticles chosen. The linearly varying wall temperature changes the flow pattern and results in a higher heat transfer rate when compared to the isothermal wall. The heat transfer coefficient ratios of (Al_2O_3) and (TiO_2) nanofluids are minimum at ($Ra=10^4$) while they are maximum for (Cu, and CuO) nanofluids. Results clearly show that the type of nanoparticles considered is very important on the convective heat transfer application.

Table 1.Thermo-physical properties of basic fluids and nanoparticles , Oztop, and Abu-Nada, [10]; Anilkumar, and Jilani , [14].

Physical properties	Base fluid	Nanoparticles			
	Ethylene glycol	Copper(Cu)	CuO	Al_2O_3	TiO_2
ρ (kg/m^3)	1116	8933	6500	3970	4250
Cp (J/kg.K)	2382	385	540	765	686.2
k (W/m.K)	0.249	401	18	40	8.9538
β x 10^{-5} (K^{-1})	65	1.67	85	0.85	0.9

Table 2. Grid independency results (Pr = 0.7, Ra=10^3)

Grid	$\square_{min}$	U_{max}
11 × 21	-1.12679	1.73129
21 × 41	-1.1628	1.80167
31 × 61	-1.17957	1.82864
41 × 81	-1.18810	1.84273

Table 3. Comparison of pure fluid solutions with previous works in an enclosure for Pr = 0.7 with different Rayleigh numbers.

Error max. (± %) for *Nu*	Tiwari and Das (2007)	K.C.Lin, A. Violi (2010)	Present study	
				$Ra=10^3$
2.25	1.087	1.118	1.112	Nu
	3.642	3.597	3.512	U_{max}
	0.804	0.819	0.801	Y
	3.703	3.690	3.516	V_{max}
	0.178	0.181	0.167	X
				$Ra=10^4$
4	2.195	2.243	2.284	Nu
	16.144	16.158	15.816	U_{max}
	0.822	0.819	0.813	Y
	19.665	19.648	18.237	V_{max}
	0.110	0.112	0.133	X
				$Ra=10^6$
1.65	8.803	8.758	8.905	Nu
	65.586	66.469	65.241	U_{max}
	0.839	0.868	0.867	Y
	219.736	222.339	220.846	V_{max}
	0.042	0.038	0.036	X

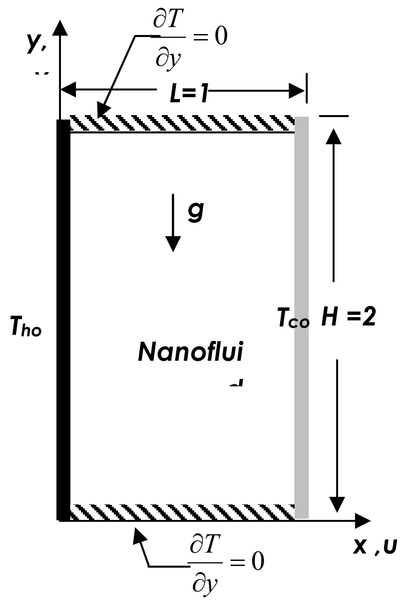

Fig.(1): Schematic for the physical model of the problem

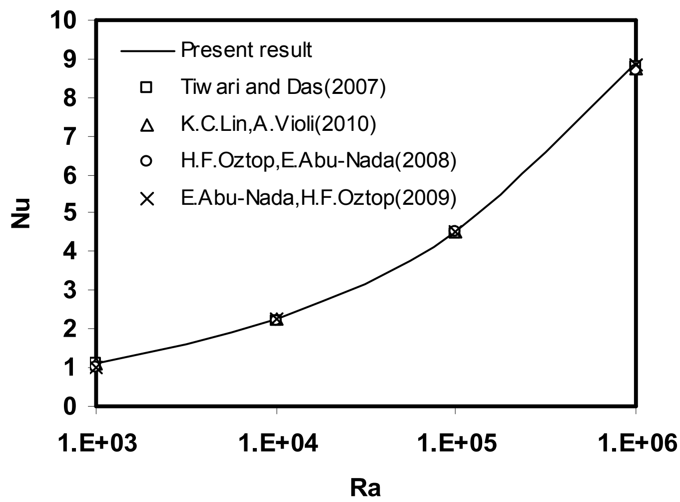

Fig. (2): Comparison between present work and other published for the mean Nusselt number versus (Ra) number for (Pr = 0.7).

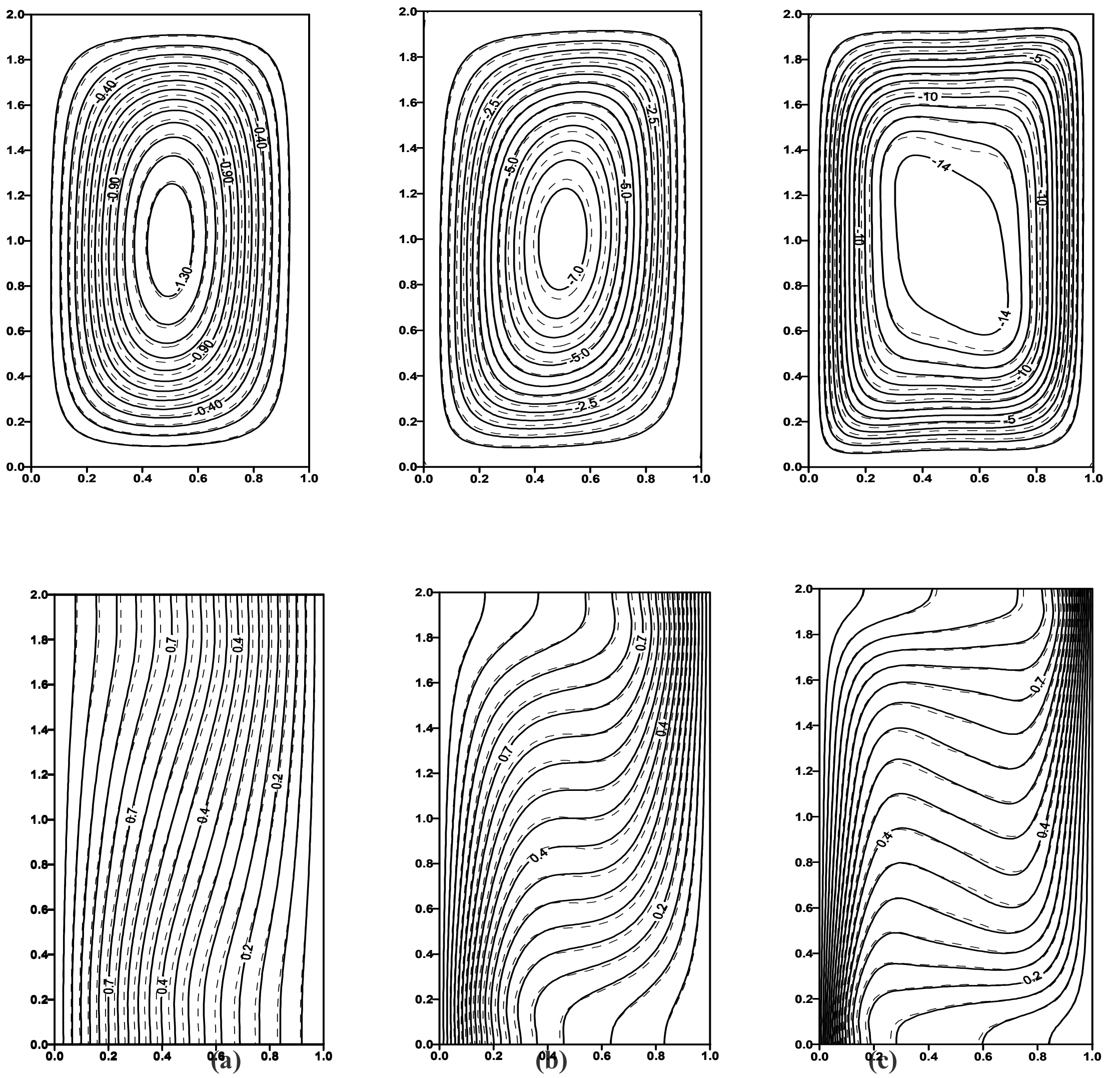

Fig. (3): Streamlines (on the top) and Isotherms (on the bottom) for CuO-EG nanofluids (- - -), pure fluid (—), □ = 0.02 (a) Ra= 10^3 (Ψ_{min}=-2.6), (b) Ra= 10^4 (Ψ_{min} =-13), and (c) Ra= 10^5 (Ψ_{min} =-22)

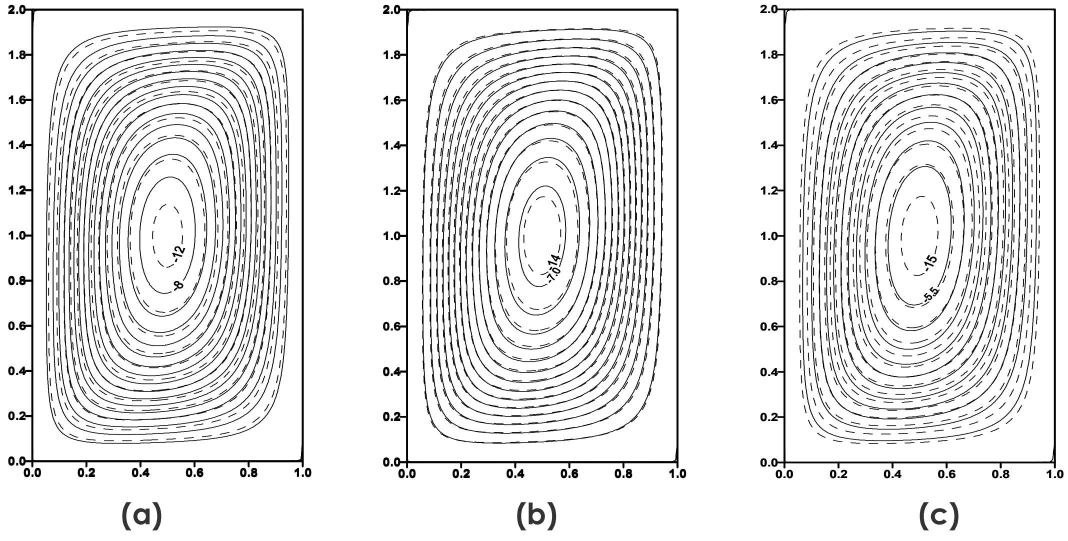

(a) **(b)** **(c)**

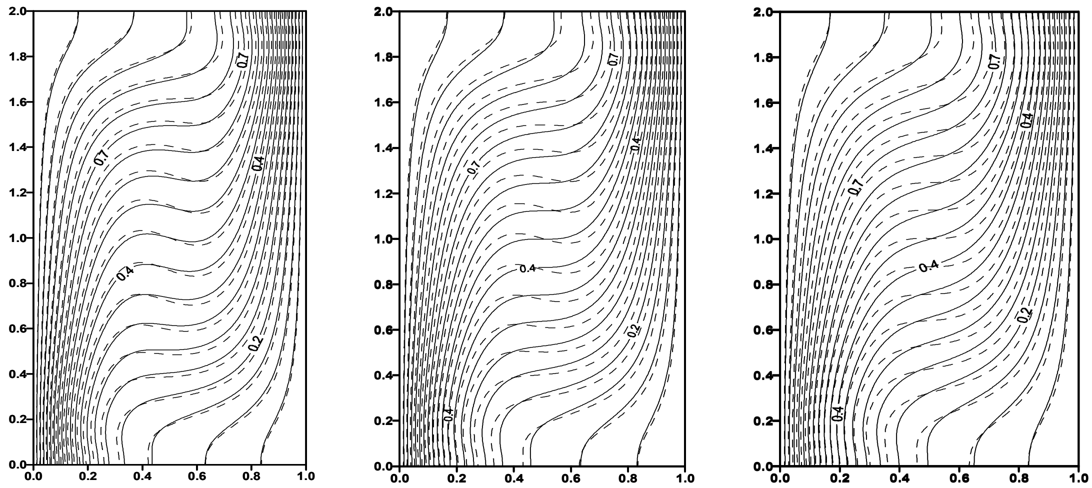

(a) (b) (c)

Fig. (4): Streamlines (on the top) and Isotherms (on the bottom) for Cu-EG nanofluids (- - -),

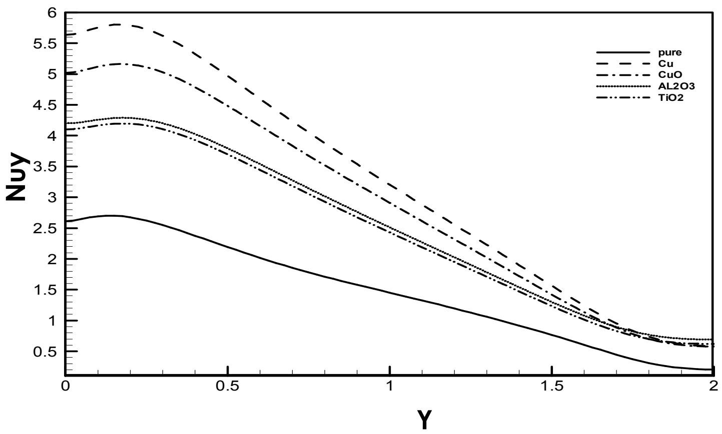

Fig. (5)Variation of local Nusselt number along the heated wall for different nanoparticles at Ra = 10^4 , ϕ = 0.04

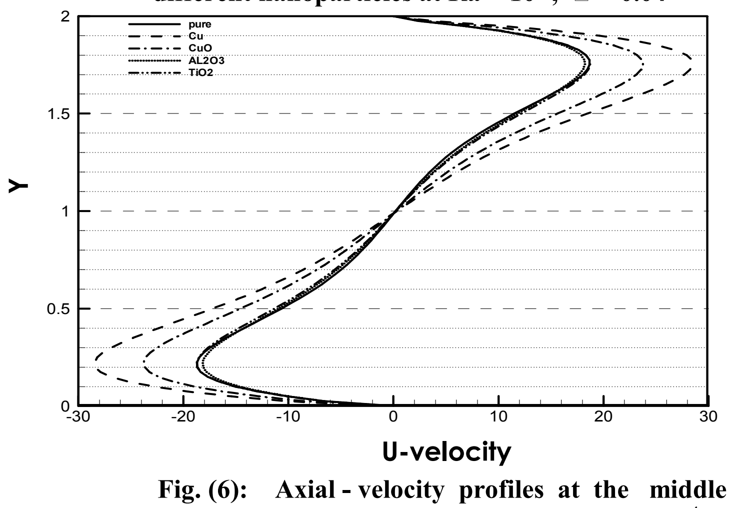

Fig. (6): Axial - velocity profiles at the middle of the enclosure for different nano-particles at Ra= 10^4 , ϕ = 0.02

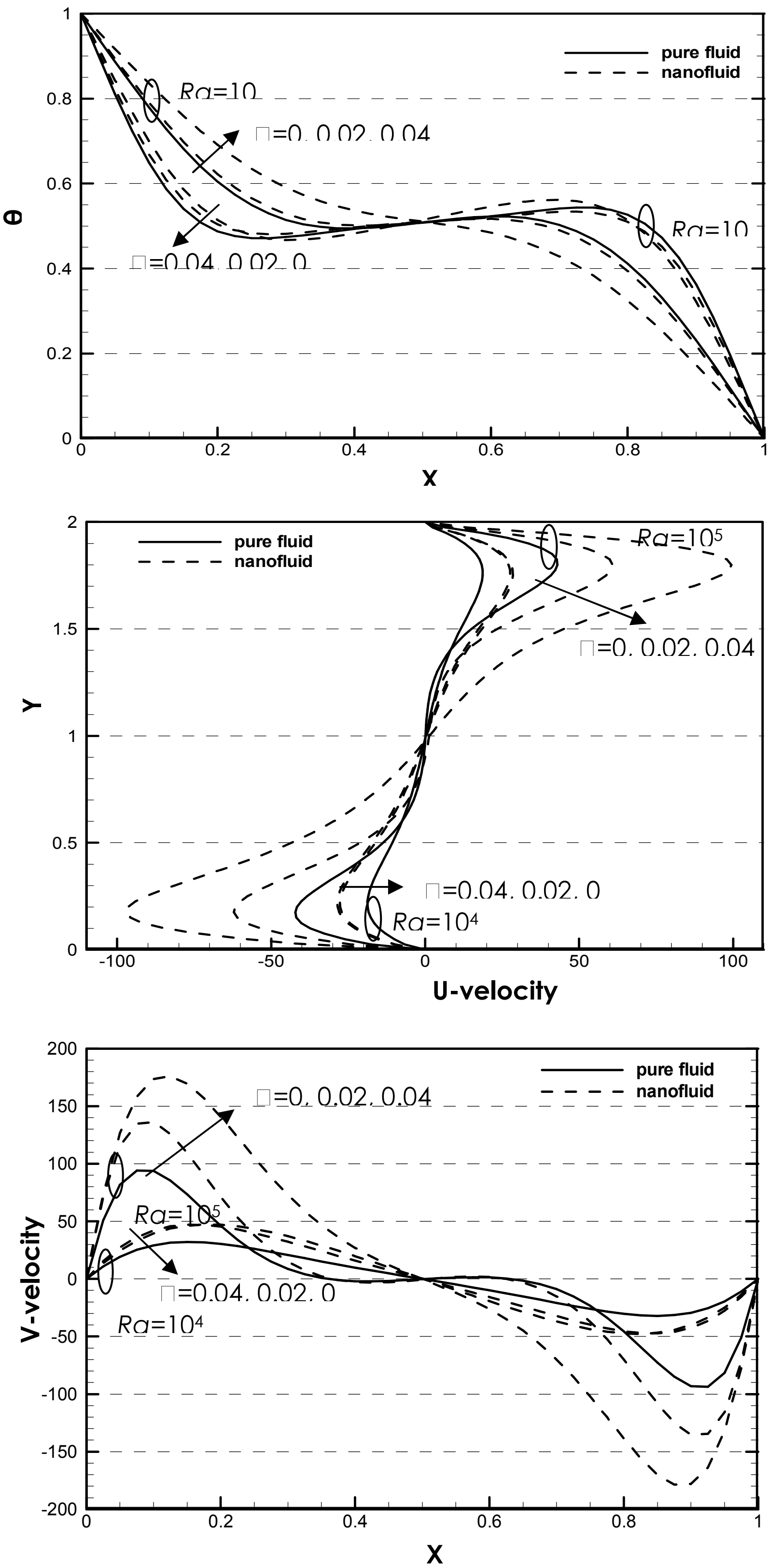

Fig. (7): Comparison of the isotherm and velocity profiles between nanofluid and pure fluid for various Rayleigh numbers (Cu-EG, □= 0.02 and 0.04).

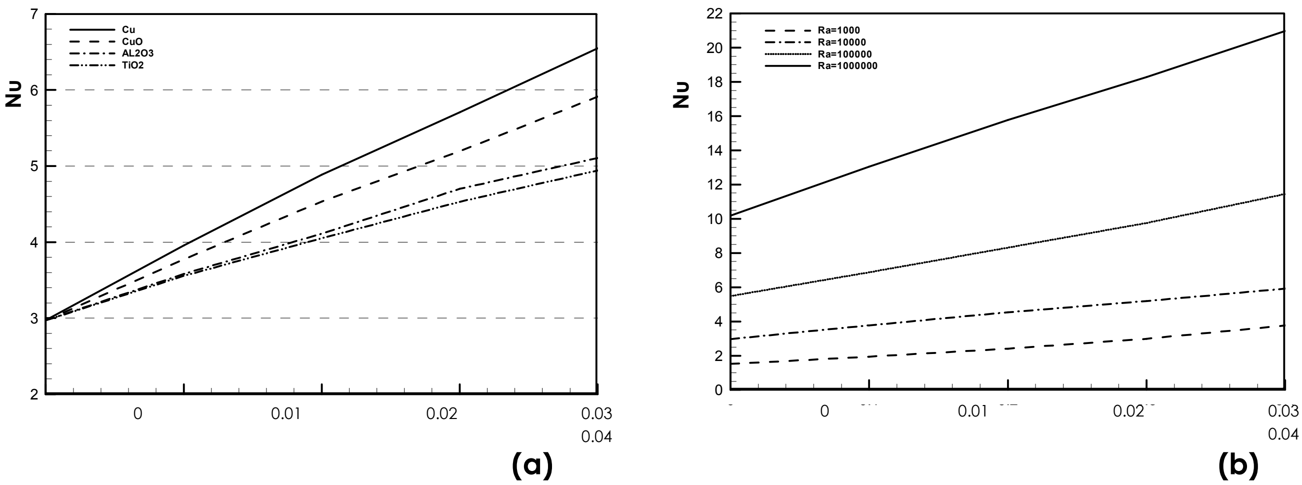

Fig. 8: Variation of mean Nusselt numbers with volume concentration (a)for different nano-particles at Ra = 10^4, (b) for CuO-EG for different (Ra) numbers

References:

1- Choi, U.S. " Enhancing thermal conductivity of fluids with nanoparticles ," in: D.A. Siginer, H.P. Wang, (Eds.), Developments and applications of non- Newtonian flows, FED-vol. 231, 66, pp. 99–105, 1995.

2- Y Xuan, Q Li, "Heat transfer enhancement of nanofluids," Int.J.HFF, vol.21, pp.58-64, 2000.

3- Dagtekin, H.F Oztop, "Natural convection heat transfer by heated partitions within enclosure,"Int.Comm.HMT, vol.28 (6), pp.823-834, 2001.

4- P Keblinski, S.R Phillpot, S.U.S Choi, J.A Eastman, "Mechanisms of heat flow in suspensions of nanosized particles (nanofluids)," Int. J. HMT, vol.45, pp.855-863, 2002.

5- Khalil Khanafer, Kambiz Vafai and MarilynLightstone, "Buoyancy-driven heat transfer enhancement in a two-dimensional enclosure utilizing nanofluids,"Int. J.HMT, vol.46, pp.3639-3653, 2003.

6- H Oztop, E Bilgen,"Natural convection in differentially heated and partially divided square cavities with internal heat generation," Int. J. Heat Fluid Flow, vol. 27, pp.466-475, 2006.

7-Hwang, K.S., Lee, Ji-Hwan, Jang, S.P. "Buoyancy-driven heat transfer of water based Al2 O3 nanofluids in a rectangular cavity". Int. J. Heat Mass Transfer 50, pp.4003–4010, 2007.

8- Jou, R.Y., Tzeng, S.C." Numerical research of nature convective heat transfer enhancement filled with nanofluids in rectangular enclosures". Int. Comm. Heat Mass Transfer 33, pp.727–736, 2006.

9- Tiwari, R.K., Das, M.K. "Heat transfer augmentation in a two-sided lid-driven differentially heated square cavity utilizing nanofluids." Int. J. Heat Mass Transfer 50, pp.2002–2018, 2007.

10- Oztop, H.F, Abu-Nada, E. "Numerical study of natural convection in partially heated rectangular enclosures filled with nanofluids" Int. J. Heat and Fluid Flow 29, pp.1326–1336, 2008.

11- Abu-Nada, E., Oztop, H.F. “Effects of inclination angle on natural convection in enclosures filled with Cu–water nanofluid.” Int. J. Heat Fluid Flow 30, pp.669–678, 2009.

12- K.C. Lin, A. Violi. “Natural convection heat transfer of nanofluids in a vertical cavity: Effects of non-uniform particle diameter and temperature on thermal conductivity”/ Int. J. Heat and Fluid Flow 31, pp.236–245, 2010.

13- H.C. Brinkman. “The viscosity of concentrated suspensions and solution”, Journal of Chemical Physics 20, pp.571–581, 1952.

14- S.H Anilkumar, G Jilani. "Natural Convection Heat Transfer Enhancement in a Closed Cavity with Partition Utilizing Nano Fluids" World Congress on Engineering (WCE) Vol II, pp.978-988, 2008.

Nomenclature:

g	gravitational acceleration (ms^{-2})	□	solid volume fraction		
H	enclosure height (m)	υ	kinematic viscosity ($m^2\ s^{-1}$)		
h	heat source length (m)	θ	dimensionless temperature		
L	enclosure width (m)	ω	vorticity (s^{-1})		
P	pressure (Pa)	Ω	dimensionless vorticity		
T	temperature (K)	ψ	dimensional stream function(m^2s^{-1})		
t	time (s)	Ψ	dimensionless stream function		
u, v	dimensional velocity components	ρ	density (kg m^{-3})		
U, V	dimensionless velocity components	μ	dynamic viscosity (kg $m^{-1}s^{-1}$)		
x, y	dimensional Cartesian coordinates	Subscripts			
X, Y	dimensionless Cartesian coordinates	co	cold	nf	nanofluid
y_p	center of location of heat source (m)	eff	effective	s	nanoparticle
Greek Symbols		f	fluid		
β	thermal expansion coefficient (K^{-1})	ho	hot		